

## Supporting Information

**Hybrid cobalt-manganese oxides prepared by ordered steps with a ternary nanosheets structure and its high performance as binder-free electrode for energy storage**

*Qingjie Lu<sup>a</sup>, Shiqiang Zhou<sup>a</sup>, Mingpeng Chen<sup>b</sup>, Bo Li<sup>a</sup>, Haitang Wei<sup>a</sup>, Baoye Zi<sup>a</sup>,  
Yumin Zhang<sup>a</sup>, Jin zhang<sup>a</sup>, Qingju Liu<sup>a\*</sup>*

---

<sup>a</sup> *Yunnan Key Laboratory for Micro/Nano Materials & Technology, National Center for International Research on Photoelectric and Energy Materials, School of Materials and Energy, Yunnan University, Kunming 650091, China*

<sup>b</sup> *University of Macau, Macau, China*

**\*Corresponding authors:**

*E-mail: qjliu@ynu.edu.cn*

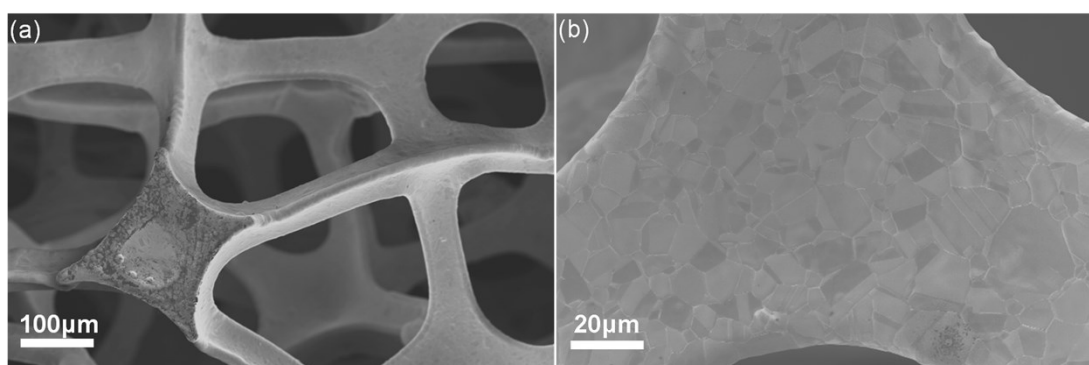


Fig. S1 (a-b) SEM images of treated nickel foam.

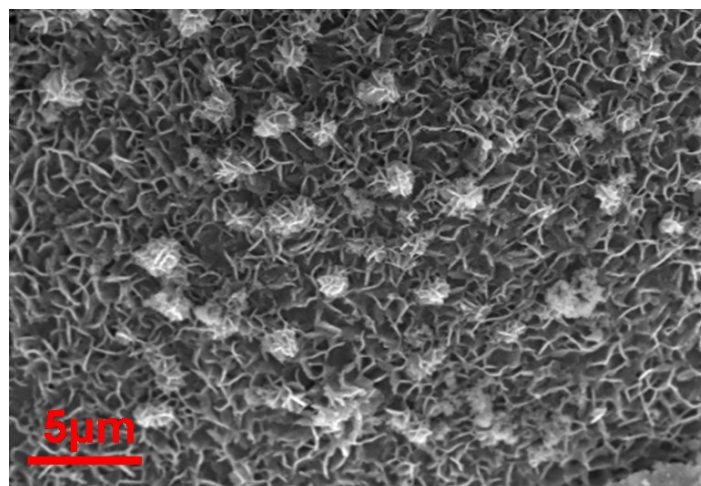


Fig. S2 SEM image of  $\text{Co}_3\text{O}_4/\text{MnO}_2$ .

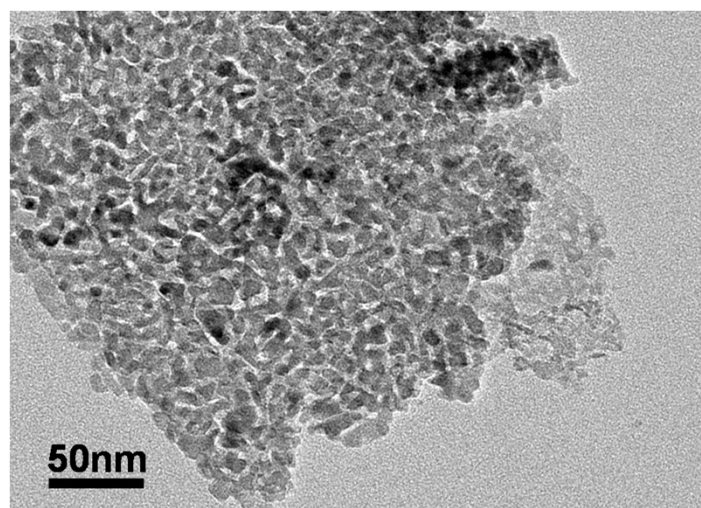


Fig. S3 TEM image of  $\text{Co}_3\text{O}_4$ .

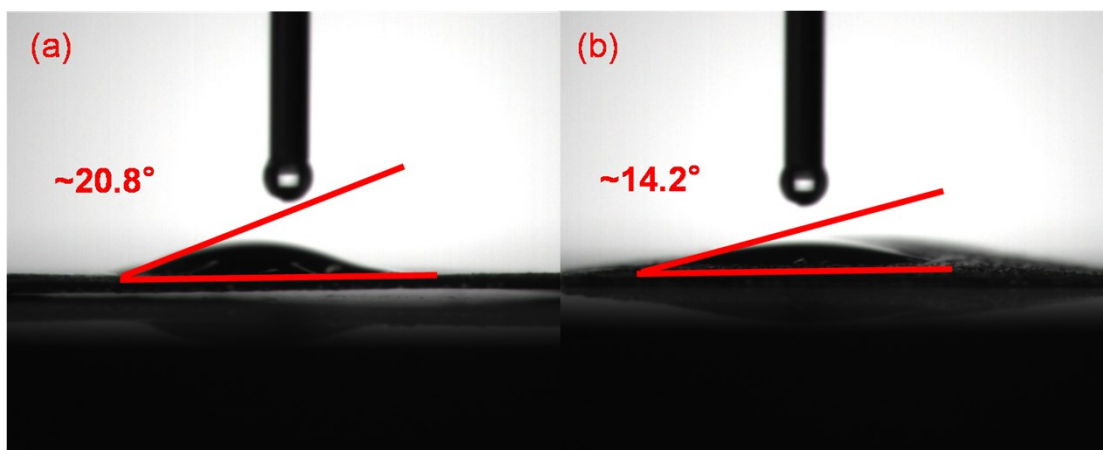


Fig. S4 Contact-angle of (a)  $\text{Co}_3\text{O}_4/\text{MnO}_2/\text{GO}$  and (b)  $\text{Co}_3\text{O}_4/\text{MnO}_2$ .

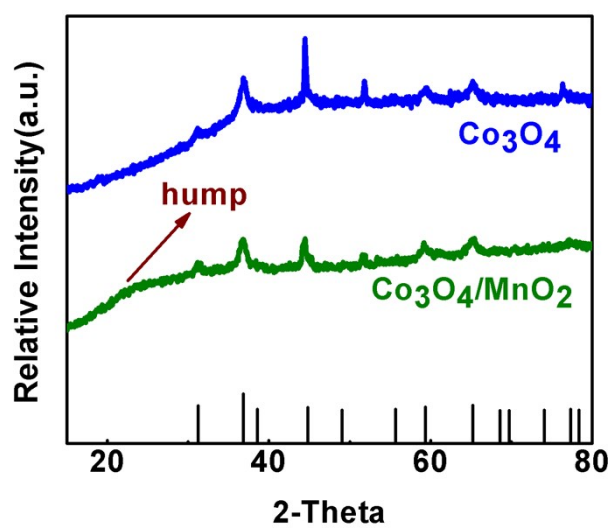


Fig. S5 XRD patterns of the samples.

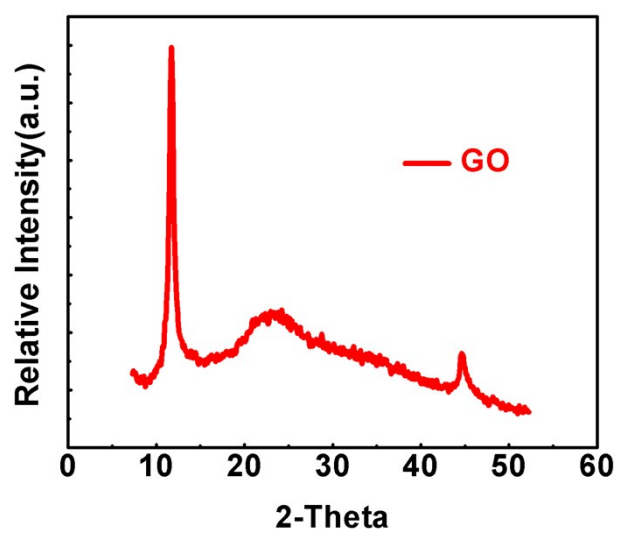


Fig. S6 XRD pattern of GO.

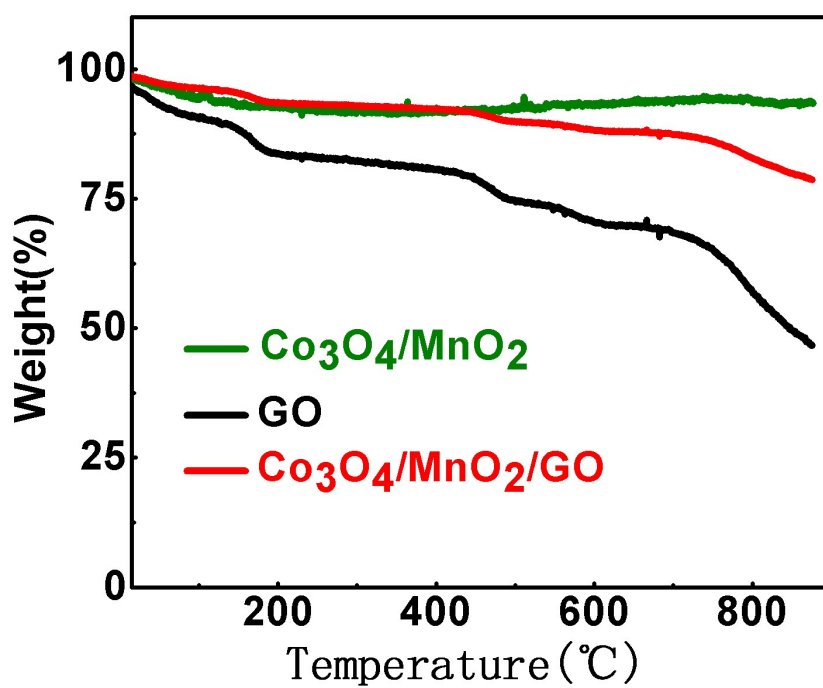


Fig. S7 TG curves of the samples.

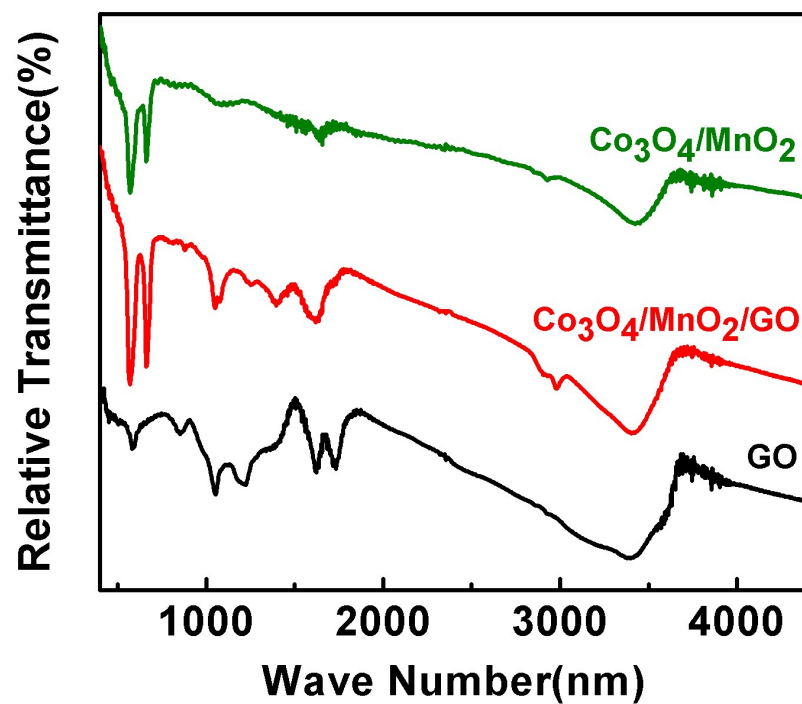


Fig. S8 FT-IR patterns of the samples.

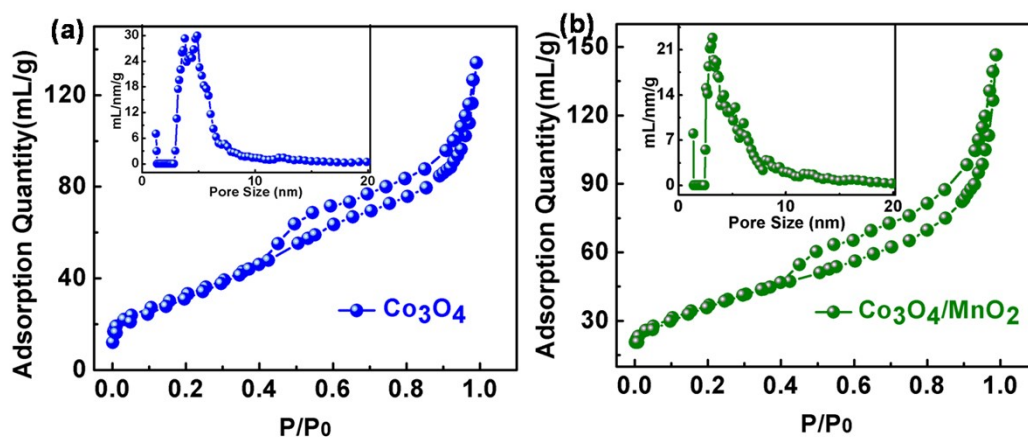


Fig. S9 (a) N<sub>2</sub> desorption/adsorption isotherms and pore size distribution of  $\text{Co}_3\text{O}_4$ . (b) N<sub>2</sub> desorption/adsorption isotherms and pore size distribution of  $\text{Co}_3\text{O}_4/\text{MnO}_2$ .

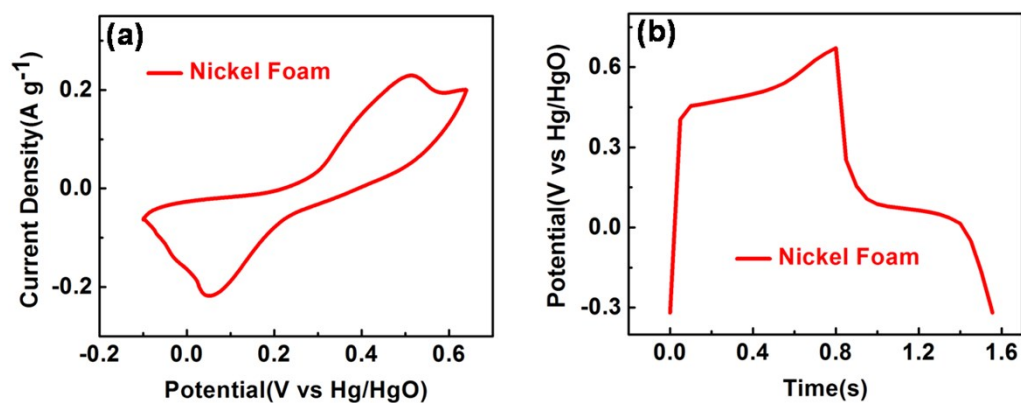


Fig. S10 CV curve at  $200 \text{ mV s}^{-1}$  and GCD curve at  $0.5 \text{ A g}^{-1}$  of the pure nickel foam.

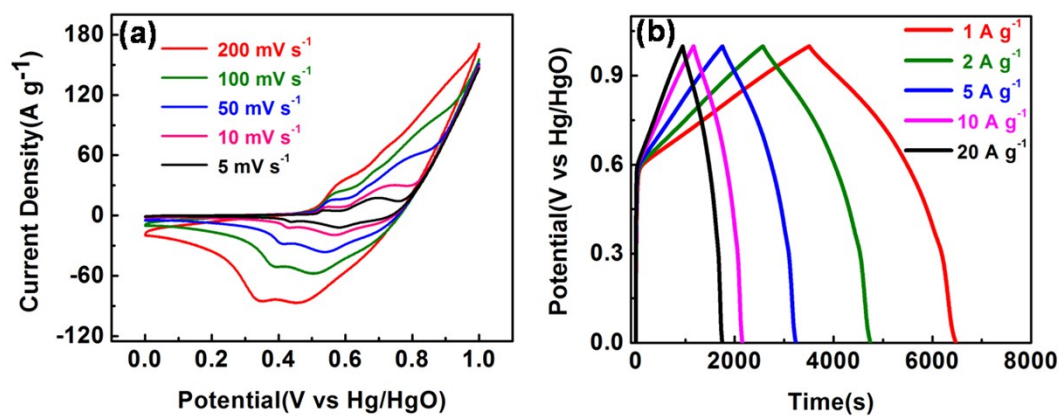


Fig. S11 (a) CV curves of  $\text{Co}_3\text{O}_4/\text{MnO}_2/\text{GO}$  electrode at different scan rates. (b) GCD curves of  $\text{Co}_3\text{O}_4/\text{MnO}_2/\text{GO}$  electrode at different current densities.

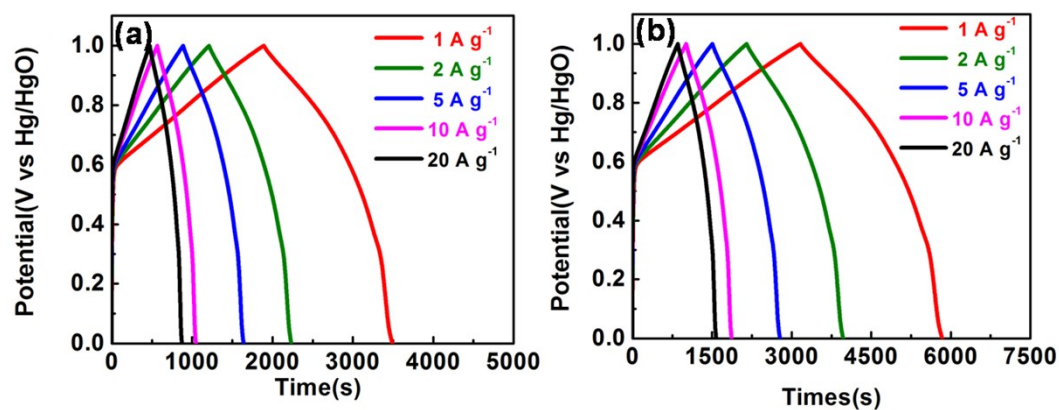


Fig. S12 (a) GCD curves of  $\text{Co}_3\text{O}_4$  electrode at different current densities. (b) GCD curves of  $\text{Co}_3\text{O}_4$  electrode at different current densities.

$\text{Co}_3\text{O}_4/\text{MnO}_2$  electrode at different current densities.

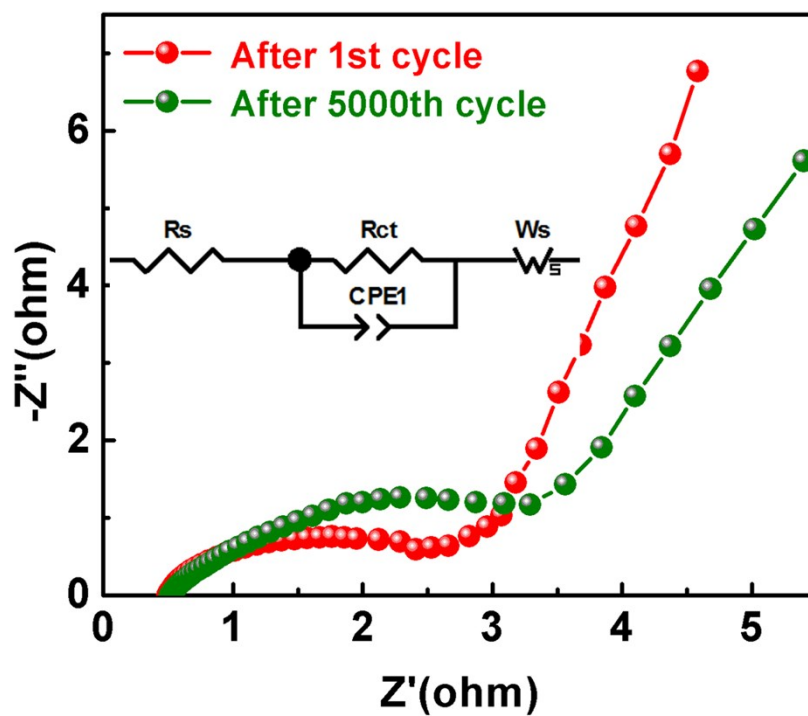


Fig. S13 Nyquist plots of  $\text{Co}_3\text{O}_4/\text{MnO}_2/\text{Go}$  binder-free electrode after 1st cycle and 5000th cycle.



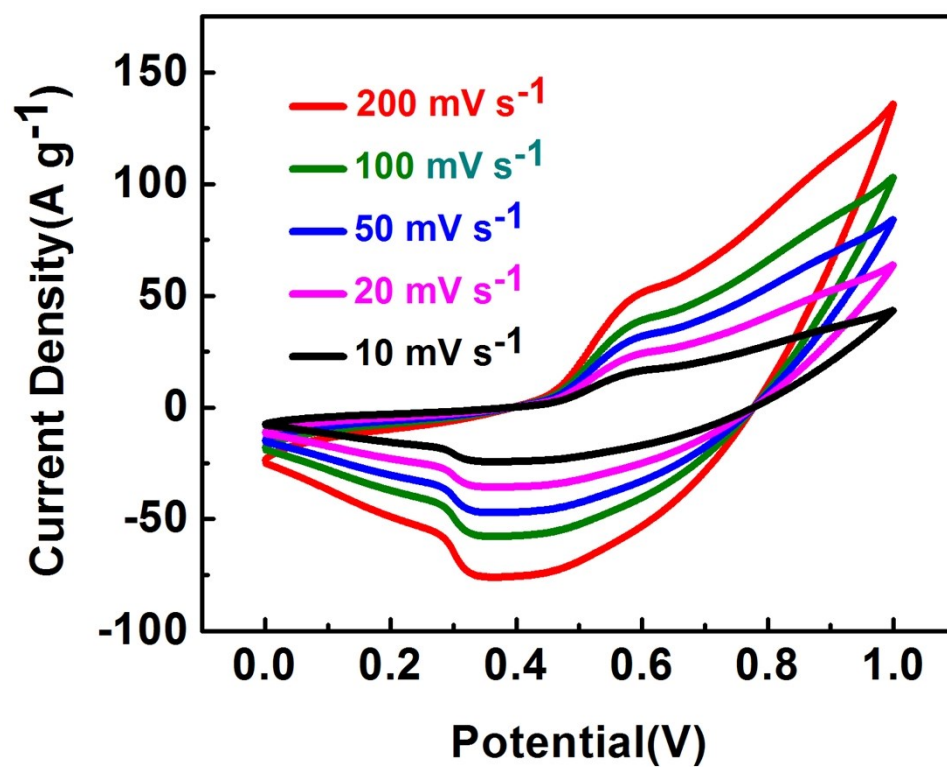


Fig. S14 CV curves of the device at different scan rates.

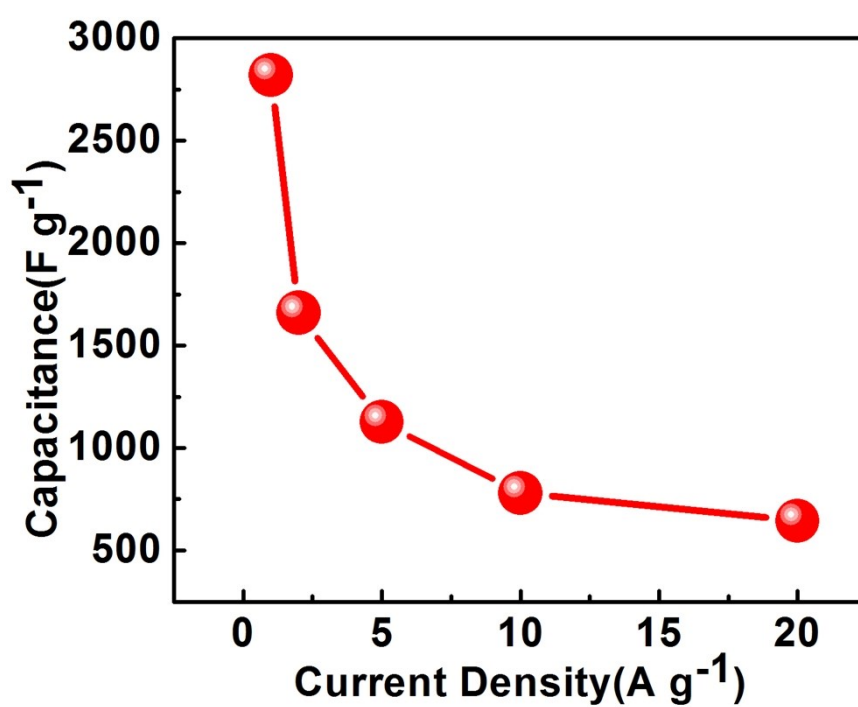


Fig. S15 Capacitance values of the device at different current densities.

Table S1. SSA and pores properties of the three samples.

Samples	SSA (m <sup>2</sup> /g)	Pore volume (cc/g)	Average pore size (nm)
Co <sub>3</sub> O <sub>4</sub>	124.17	0.21	6.68
Co <sub>3</sub> O <sub>4</sub> /MnO <sub>2</sub>	141.87	0.23	6.93
Co <sub>3</sub> O <sub>4</sub> /MnO <sub>2</sub> /GO	140.15	0.22	7.07

Table S2. Resistance values of the samples.

Samples	Rs (Ω)	Rct (Ω)	Ws (Ω)
Co <sub>3</sub> O <sub>4</sub>	0.4	2.36	8.57
Co <sub>3</sub> O <sub>4</sub> /MnO <sub>2</sub>	0.54	2.18	9.08
Co <sub>3</sub> O <sub>4</sub> /MnO <sub>2</sub> /GO	0.49	1.45	5.82